ture in vivo. So far, there is no evidence that tumors can stimulate the growth of new lymphatic vessels (*23*), but further studies should establish the role of VEGF-C in lymphangiomas and in tumor metastasis via the lymphatic vasculature as well as in various other disorders involving the lymphatic system and their treatment.

REFERENCES AND NOTES

1. N. Ferrara and T. Davis-Smyth, *Endocr. Rev.*, in press.
2. B. Olofsson *et al.*, *Proc. Natl. Acad. Sci. U.S.A.* **93**, 2576 (1996); S. Grimmond *et al.*, *Genome Res.* **6**, 124 (1996).
3. V. Joukov *et al.*, *EMBO J.* **15**, 290 (1996); J. Lee *et al.*, *Proc. Natl. Acad. Sci. U.S.A.* **93**, 1988 (1996).
4. E. Kukk *et al.*, *Development* **122**, 3829 (1996).
5. D. Maglione, V. Guerriero, G. Viglietto, P. Delli-Bovi, M. G. Persico, *Proc. Natl. Acad. Sci. U.S.A.* **88**, 9267 (1991).
6. M. Klagsbrun and P. A. D'Amore, *Cytokine Growth Factor Rev.* **7**, 259 (1996).
7. The human VEGF-C cDNA (GenBank accession number X94216) was blunt-end ligated to the Bam HI restriction site of the K14 expression cassette (*8*), and an Eco RI–Hind III fragment containing the K14 promoter, VEGF-C cDNA, and K14 polyadenylation signal was isolated and injected into fertilized oocytes of the FVB/NIH strain of mice. The injected zygotes were transplanted into oviducts of pseudopregnant C57BL/6 × DBA/2J hybrid mice. We analyzed the resulting founder mice for the presence of the transgene by polymerase chain reaction of tail DNA, with the primers: 5′-CATGTACGAACCGCCAG-3′ and 5′-AATGACCAGAGAGAGGCGAG-3′. The tail DNAs were also subjected to endonuclease digestion, Southern blotting, and hybridization analysis using the transgene fragment as the probe.
8. R. Vassar, M. Rosenberg, S. Ross, A. Tyner, E. Fuchs, *Proc. Natl. Acad. Sci. U.S.A.* **86**, 1563 (1989).
9. H. J. Leu and J. T. Lie, in *Vascular Pathology* (Chapman & Hall, London, 1995), p. 509.
10. T. W. Fossum and M. W. Miller, *J. Vet. Intern. Med.* **6**, 283 (1992).
11. L. V. Leak, *Microvasc. Res.* **2**, 361 (1970).
12. Y. Muragaki *et al.*, *Proc. Natl. Acad. Sci. U.S.A.* **92**, 8763 (1995); M. Rehn and T. Pihlajaniemi, *ibid*. **91**, 4234 (1994).
13. M. Jeltsch *et al.*, data not shown.
14. M. Schmelz, R. Moll, C. Kuhn, W. W. Franke, *Differentiation* **57**, 97 (1994).
15. K. Pajusola *et al.*, *Cancer Res.* **52**, 5738 (1992); F. Galland *et al.*, *Oncogene* **8**, 1233 (1993).
16. B. I. Terman *et al.*, *Biochem. Biophys. Res. Commun.* **187**, 1579 (1992); B. Millauer *et al*., *Cell* **72**, 83 (1993).
17. J. Korhonen, A. Polvi, J. Partanen, K. Alitalo, *Oncogene* **9**, 395 (1994).
18. A. Kaipainen *et al.*, *Proc. Natl. Acad. Sci. U.S.A.* **92**, 3566 (1995).
19. T. Yamaguchi, D. Dumont, R. Conion, M. Breitman, J. Rossant, *Development* **118**, 489 (1993); D. Dumont *et al.*, *Dev. Dyn.* **203**, 80 (1995).
20. J. Folkman and Y. J. Shing, *J. Biol. Chem.* **267**, 10931 (1992).
21. A. J. Leu, D. A. Berk, F. Yuan, R. K. Jain, *Am. J. Physiol.* **267**, 1507 (1994); M. A. Swartz, D. A. Berk, R. K. Jain, *ibid.* **270**, 324 (1996).
22. V. Joukov, unpublished data.
23. J. Folkman, *N. Engl. J. Med.* **334**, 921 (1996).
24. D. Fukumura *et al.*, *Cancer Res.* **55**, 4824 (1995).
25. For electron microscopy, tissue pieces from two transgenic skin biopsies were fixed in formaldehyde, postfixed in 2% osmium tetroxide, and embedded in LX 112. Sagittal ultrathin sections were studied with the Jeol1200EX electron microscope.
26. For immunohistochemistry, we stained cryostat sections of 5 to 10 μm from abdominal and back skin with anti-mouse desmoplakin I and II monoclonal antibodies (Progen), affinity-purified rabbit anti-mouse collagen XVIII IgG (a gift from T. Pihlajaniemi), and rabbit anti-mouse laminin IgG (provided by E. Lehtonen), by using the Vectastain ABC Elite kit (Vector Laboratories). Normal mouse or rabbit sera were used as negative controls for the stainings.
27. In situ hybridization of sections was performed as described [A. Kaipainen *et al.*, *J. Exp. Med.* **178**, 2077 (1993)]. The human VEGF-C antisense RNA probe was generated from linearized pCR™II plasmid (Invitrogen) containing an Eco RI fragment corresponding to nucleotides 628 through 1037 of human VEGF-C cDNA. The VEGFR-3 probe was described earlier (*18*). The VEGFR-2 probe was an Eco RI fragment covering base pairs 1958 through 2683 (GenBank accession number X59397, a gift from J. Rossant).
28. For measurement of DNA synthesis, small (3 mm by 3 mm) skin biopsies from four transgenic and four control mice were incubated in Dulbecco's modification of Eagle's medium with 10 μg/ml BrdU for 6 hours at 37°C, fixed in 70% ethanol for 12 hours, and embedded in paraffin. After a 30-min treatment with 0.1% pepsin in 0.1 M HCl at room temperature to denature DNA, staining was carried out as above with mouse monoclonal antibodies to BrdU (Amersham).
29. Fluorescence microlymphography was performed as follows. The staining of the lymphatic network in vivo was carried out as described (*20*). Briefly, 8-week-old mice were anesthetized and placed on a heating pad to maintain a 37°C temperature. A 30-gauge needle, connected to a catheter filled with a solution of FITC-dextran (2 M, 8 mg/ml in phosphate-buffered solution), was injected intradermally into the tip of the tail. The solution was infused with a constant hydrostatic pressure equivalent to a 50-cm column of water (flow rate averaging roughly 0.01 μl/min) until the extent of network filling remained constant (approximately 2 hours). Flow rate and fluorescence intensity were monitored continuously throughout the experiment. The intravital fluorescence microscopy of blood vessels was as described (*24*).

30. We thank E. Saksela for help with histological interpretation; E. Lehtonen for help in electron microscopy; E. Hatva for critical reading of the manuscript; E. Fuchs for the K14 expression cassette; and E. Koivunen, M. Helanterä, T. Tainola, and E. Rose for excellent technical assistance. Supported through the Finnish Cancer Organizations, the Finnish Academy, the Sigrid Juselius Foundation, the University of Helsinki, the State Technology Development Centre, and NIH.

22 January 1997; accepted 27 March 1997

Geometric Control of Cell Life and Death

Christopher S. Chen, Milan Mrksich, Sui Huang, George M. Whitesides, Donald E. Ingber*

Human and bovine capillary endothelial cells were switched from growth to apoptosis by using micropatterned substrates that contained extracellular matrix-coated adhesive islands of decreasing size to progressively restrict cell extension. Cell spreading also was varied while maintaining the total cell-matrix contact area constant by changing the spacing between multiple focal adhesion-sized islands. Cell shape was found to govern whether individual cells grow or die, regardless of the type of matrix protein or antibody to integrin used to mediate adhesion. Local geometric control of cell growth and viability may therefore represent a fundamental mechanism for developmental regulation within the tissue microenvironment.

The local differentials in cell growth and viability that drive morphogenesis in complex tissues, such as branching capillary networks (*1*, *2*), are controlled through modulation of cell binding to extracellular matrix (ECM) (*3*–*6*). Local disruption of ECM by pharmacologic or genetic means results in selective programmed cell death (apoptosis) within adjacent cells (*2*, *6*, *7*). Soluble integrin $\alpha_V\beta_3$ antagonists also induce apoptosis in cultured endothelial cells and promote capillary involution in vivo (*8*). Furthermore, death can be prevented by allowing suspended cells to attach to immobilized antibodies to integrins or by inhibiting tyrosine phosphatases (*7*, *9*). For these reasons, adhesion-dependent control of apoptosis has been assumed to be mediated by changes in integrin signaling. Analysis of capillary regression in vivo, however, has revealed that dying capillary cells remain in contact with ECM fragments, thus suggesting that the cell foreshortening caused by ECM dissolution may be the signal that initiates the death program (*2*). This possibility is supported by the finding that endothelial cells spread and grow on large (>100-μm diameter) microcarrier beads (*4*), whereas they rapidly die when bound to small (4.5 μm) ECM-coated beads (*10*) that cluster integrins and activate signaling but do not support cell extension (*11*).

Understanding how this apoptotic switch is controlled in capillary cells has enormous clinical implications, because angiogenesis is a prerequisite for tumor growth (*12*). Thus, we set out to determine whether cell shape or integrin binding per se governs life and death in these cells. We first measured apoptosis rates in suspended

C. S. Chen, S. Huang, D. E. Ingber, Departments of Surgery and Pathology, Children's Hospital–Harvard Medical School, Enders 1007, 300 Longwood Avenue, Boston, MA 02115, USA.
M. Mrksich and G. M. Whitesides, Department of Chemistry, Harvard University, Cambridge, MA 02138, USA.

*To whom correspondence should be addressed. E-mail: ingber@a1.tch.harvard.edu

human capillary endothelial cells attached to a range of different-sized beads coated with fibronectin (FN). Most cells survived when spread on FN-coated planar dishes in medium that contained saturating amounts of growth factors, whereas about 60% of nonadherent cells entered the death program within 24 hours (Fig. 1, A and B). In contrast, fewer than 10% of cells adherent to large (>25 μm) FN-coated beads underwent programmed cell death. Unlike suspended cells, which remained small and spherical, these cells and their nuclei appeared to flatten as they extended around the beads (Fig. 1A). Importantly, as the bead diameter was decreased to 10 μm, cells became more rounded, and the apoptotic index increased to match that in nonadherent cells (Fig. 1B).

The size of these spherical beads affects not only the degree of cell and nuclear spreading but also ECM curvature and bead internalization. The 10-μm beads appeared fully engulfed by cells within 4 hours, whereas the 25-μm beads were never fully internalized. To eliminate these complicating factors, we used a microscale patterning technique (*13, 14*) to fabricate planar adhesive islands of defined size and shape, separated by nonadhesive regions. When plated on circular FN-coated islands 10 or 20 μm in diameter, cells spread until they took on the size and shape of the underlying adhesive island (Fig. 1C). Significantly more cells entered apoptosis when held in a round form on 20-μm circles than when spread on identically fabricated unpatterned substrates (Fig. 1D). Furthermore, the subtle decrease in cell and nuclear spreading observed in cells on 10- compared with 20-μm islands (Fig. 1C) was also accompanied by a statistically significant increase in apoptosis (Fig. 1D).

Capillary cell spreading on ECM also has been shown to modulate cell cycle progression (*4, 11, 15*). To determine the precise spreading requirements for survival rather than growth, we cultured cells synchronized in the quiescent phase of the cell cycle on different-sized FN-coated adhesive islands. The different-sized islands were contained within a single substrate (Fig. 2A) to rule out the possibility that changes in cell behavior could be due to the release of paracrine growth modulators. When we plated cells on square-shaped islands coated with FN, square-shaped cells were produced that closely matched the size and shape of the adhesive island (Fig. 2A). Apoptosis progressively declined when the island size was increased from 75 to 3000 μm^2, whereas DNA synthesis was concomitantly switched on as cell and nuclear spreading were promoted (Fig. 2B).

These results demonstrate that increased cell spreading on a homogeneous, high-density coating of FN leads to cell survival and growth. However, the total area of cell-ECM contact also increases under these conditions, so integrin binding, focal adhesion formation, and accessibility to matrix-bound growth factors (*16*) may all vary in parallel. To explore this mechanism more fully, we evaluated apoptosis and

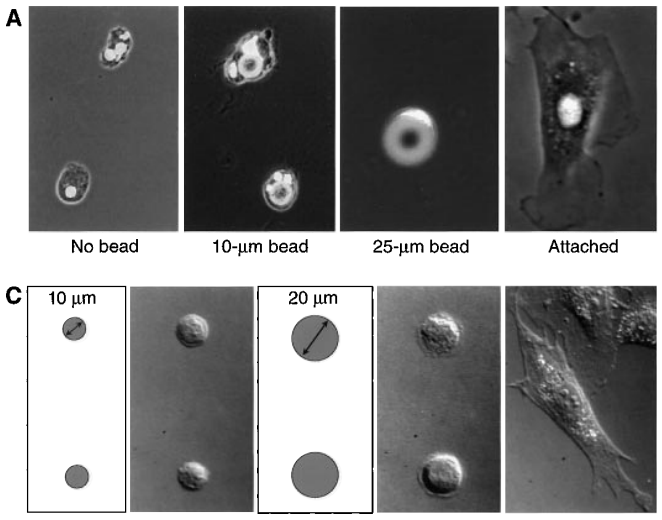

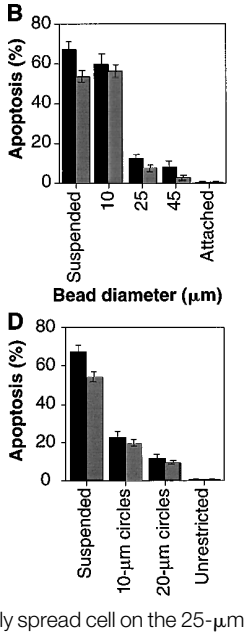

Fig. 1. Effect of cell spreading on apoptosis. (**A**) Combined phase contrast–fluorescence micrographs of capillary endothelial cells cultured in suspension in the absence or presence of different-sized microbeads or attached to a planar culture dish coated with FN for 24 hours (*28*). In the highly spread cell on the 25-μm bead, only the flattened 4′,6′-diamidino-2-phenylindole (DAPI)–stained nucleus is clearly visible. (**B**) Apoptosis in cells attached to different-sized beads, in suspension, or attached to a dish. The apoptotic index was quantitated by measuring the percentage of cells exhibiting positive TUNEL staining (black bars) (Boehringer Mannheim), which detects DNA fragmentation; similar results were obtained by analyzing changes in nuclear condensation and fragmentation in cells stained with DAPI at 24 hours (gray bars). Apoptotic indices were determined only within single cells bound to single beads. Error bars indicate SEM. (**C**) Differential interference-contrast micrographs of cells plated on substrates micropatterned with 10- or 20-μm-diameter circles coated with FN (left), by a microcontact printing method (*29*) or on a similarly coated unpatterned substrate (right). (**D**) Apoptotic index of cells attached to different-sized adhesive islands coated with a constant density of FN for 24 hours; similar results were obtained with human and bovine capillary endothelial cells (*28*). Bars same as in (B).

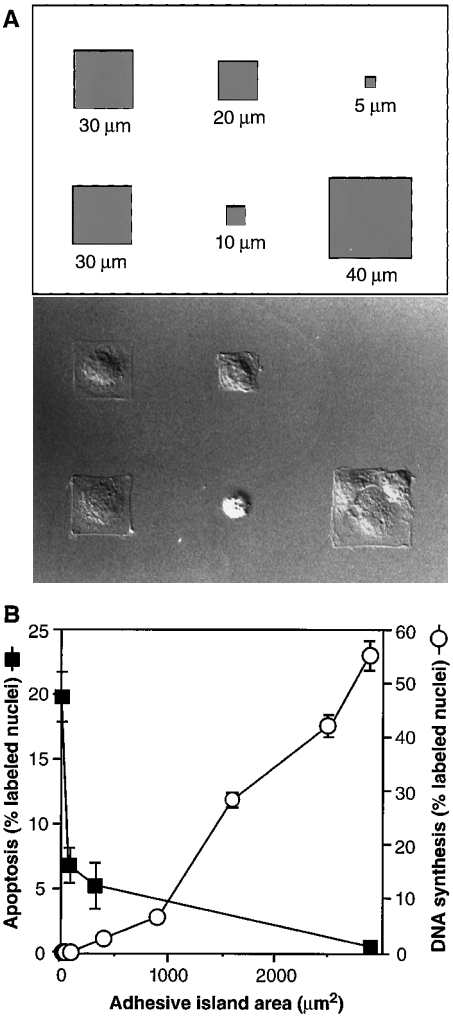

Fig. 2. Effect of spreading on cell growth and apoptosis. (**A**) Schematic diagram showing the initial pattern design containing different-sized square adhesive islands and Nomarski views of the final shapes of bovine adrenal capillary endothelial cells adherent to the fabricated substrate. Distances indicate lengths of the square's sides. (**B**) Apoptotic index (percentage of cells exhibiting positive TUNEL staining) and DNA synthesis index (percentage of nuclei labeled with 5-bromodeoxyuridine) after 24 hours, plotted as a function of the projected cell area. Data were obtained only from islands that contained single adherent cells; similar results were obtained with circular or square islands and with human or bovine endothelial cells.

growth in single cells spread across multiple, closely spaced adhesive islands of either 3 or 5 μm in diameter to approximate the size of individual focal adhesions (Fig. 3, A and B). Cell bodies spread across the intervening nonadhesive areas of the substrate, stretching processes from one small adhesive island to another. Immunofluorescence staining confirmed that adherent cells attached and formed vinculin-containing focal adhesions only on the engineered islands (Fig. 3C). By changing the spacing between adhesive islands, we could increase cell spreading 10-fold without significantly altering the total cell-ECM contact area (Fig. 3D). On these substrates, DNA synthesis scaled directly with projected cell area and not with cell-ECM contact area (Fig. 3D). Apoptosis was similarly switched off by cell spreading, even though the cell-ECM contact area remained constant under these conditions (Fig. 3D). Thus, cell shape per se appears to be the critical determinant that switches cells between life and death and between proliferation and quiescence.

In vivo studies demonstrate that programmed cell death and capillary regression can be induced by inhibiting integrin $\alpha_V\beta_3$ binding, whereas apoptosis can be prevented in vitro by attachment of cells to immobilized antibodies to integrin β_1 (anti-β_1) (*8, 9*). Because cell binding to FN is mediated by both β_1 and β_3 integrins, we chose to explore their role in shape-dependent control of apoptosis. We coated unpatterned substrates and 20-μm circular islands with antibodies specific for β_1 or $\alpha_V\beta_3$ integrins, FN, or physiological ECM ligands that preferentially use integrin β_1 (type I collagen) or $\alpha_V\beta_3$ (vitronectin). Apoptosis was greatly inhibited relative to the 60% level observed in suspended cells when cells spread on unpatterned substrates regardless of the integrin ligand used (Fig. 4). However, survival was consistently greater in cells that adhered to intact ECM proteins. When spreading was restricted by use of 20-μm circles, cells adherent to integrin β_1 ligands (FN, type I collagen, anti-β_1, or anti-β_1 combined with anti-$\alpha_V\beta_3$) exhibited much greater increases in apoptosis compared with those on either intact vitronectin or on anti-$\alpha_V\beta_3$ alone (Fig. 4). This was due to a change in sensitivity, rather than a lack of response, because similar high levels of apoptosis were induced when cell spreading was further restricted by plating on 10-μm circular islands. Thus, although geometric switching between growth and apoptosis is a general phenomenon, different adhesion receptors appear to be able to convey distinct death signals and thereby tune the cellular response to shape distortion.

The mechanism by which cells transduce changes in cell geometry into different biochemical responses remains unclear. The specialized cytoskeletal structure, or focal adhesion complex, that forms intracellularly at the site of integrin binding is a molecular bridge that mechanically couples integrins, and hence ECM, to the actin cytoskeleton (*17–19*). Because focal adhesions also orient much of the signal transduction machinery of the cell (*20*), they may integrate mechanical signals associated with changes in cell shape with chemical signals elicited directly by integrin binding and thereby modulate downstream signaling (*21*). In fact, constitutive activation of the tyrosine kinase, pp125^{FAK}, in the focal adhesion complex can lead to shape- and adhesion-independent cell survival and growth (*22, 23*). Alternatively, growth and viability may be altered directly by mechanical stress-dependent changes in the organization or stiffness of the cytoskeleton and nucleus (*18, 19, 21, 24*). For example, the increased flexibility of the cytoskeleton that has been observed in rounded cells (*18*) may permit intracellular structural rearrangements that are lethal, including the characteristic structural degeneration of the cell and nucleus that are hallmarks of apoptosis. The finding that cell survival is more tightly coupled to cell shape in cells adherent to ligands for integrin β_1 compared with integrin $\alpha_V\beta_3$ is also consistent with the observation that β_1 provides stronger ECM anchoring to resist cytoskeletal tension (*18*). From this perspective, adhesive substrates may prevent cell death and promote growth by resisting contractile forces transmitted across integrins, thereby mechanically stabilizing the nucleocytoskeletal lattice.

During morphogenesis, growing, quiescent, and dying cells often co-exist within the same microenvironment (*1, 2*). In fact, the establishment of local differentials in cell growth and viability drives pattern formation. Our results suggest that living cells can filter the same set of chemical inputs (activation of integrin and growth factor receptor signaling) to produce different functional outputs (growth versus apoptosis) as a result of local mechanical deformation of the cell or nucleus. By sensing their degree of extension or compression, cells therefore may be able to monitor local changes in cell crowding or ECM compli-

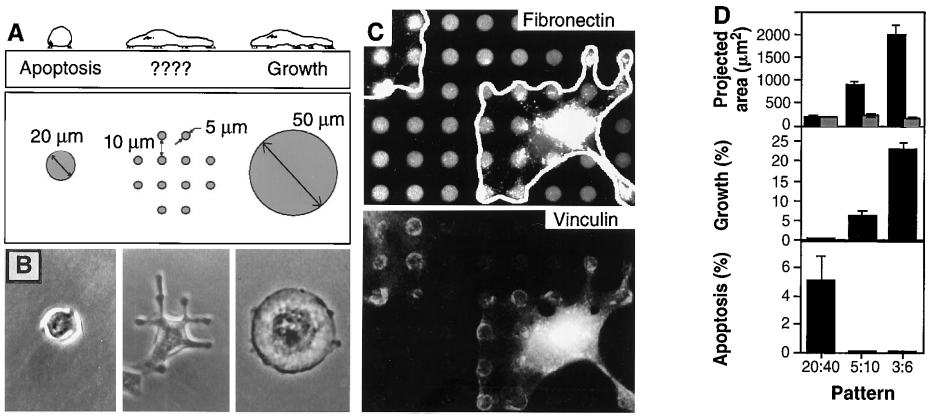

Fig. 3. Cell-ECM contact area versus cell spreading as a regulator of cell fate. (**A**) Diagram of substrates used to vary cell shape independently of the cell-ECM contact area. Substrates were patterned with small, closely spaced circular islands (center) so that cell spreading could be promoted as in cells on larger, single round islands, but the ECM contact area would be low as in cells on the small islands. (**B**) Phase-contrast micrographs of cells spread on single 20- or 50-μm-diameter circles or multiple 5-μm circles patterned as shown in (A). (**C**) Immunofluorescence micrographs of cells on a micropatterned substrate stained for FN (top) and vinculin (bottom). White outline indicates cell borders; note circular rings of vinculin staining, which coincide precisely with edges of the FN-coated adhesive islands. (**D**) Plots of projected cell area (black bars) and total ECM contact area (gray bars) per cell (top), growth index (middle), and apoptotic index (bottom) when cells were cultured on single 20-μm circles or on multiple circles 5 or 3 μm in diameter separated by 40, 10, and 6 μm, respectively.

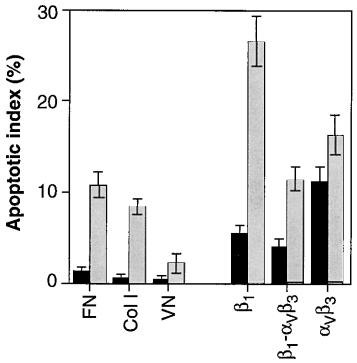

Fig. 4. Role of different integrin ligands in cell shape–regulated apoptosis. Apoptotic indices (percentage positive TUNEL staining) for cells cultured for 24 hours on unpatterned substrates (black bars) or on 20-μm circles (gray bars) coated with FN, type I collagen (Col I), vitronectin (VN), anti-β_1, anti-$\alpha_V\beta_3$, or antibodies to both integrin β_1 and integrin $\alpha_V\beta_3$ (*29*).

ance (for example, due to enhanced ECM remodeling or local application of cell tension) and thereby couple changes in ECM extension to expansion of cell mass within the local tissue microenvironment. Tissue involution may be promoted in other microenvironments by inducing rapid breakdown of ECM and associated cell retraction. During malignant transformation, progressive loss of shape-dependent regulation also may lead to cell survival in the absence of ECM extension, unrestricted mass expansion, and hence neoplastic disorganization of tissue architecture (*25–27*).

REFERENCES AND NOTES

1. E. R. Clark and E. L. Clark, *Am. J. Anat.* **64**, 251 (1938).
2. D. E. Ingber, J. A. Madri, J. Folkman, *Endocrinology* **119**, 1768 (1986).
3. D. E. Ingber and J. Folkman, *Cell* **58**, 308 (1989); C. D. Roskelley, A. Srebrow, M. J. Bissell, *Curr. Opin. Cell Biol.* **7**, 736 (1995).
4. D. E. Ingber and J. M. Folkman, *J. Cell Biol.* **109**, 317 (1989).
5. M. S. Wicha, L. A. Liotta, B. K. Vonderhaar, W. R. Kidwell, *Dev. Biol.* **80**, 253 (1980); C. J. Drake, D. A. Cheresh, C. D. Little, *J. Cell Sci.* **108**, 2655 (1995).
6. C. J. Sympson *et al*., *J. Cell Biol.* **125**, 681 (1994).
7. N. Boudreau, C. J. Sympson, Z. Werb, M. J. Bissell, *Science* **267**, 891 (1995).
8. P. C. Brooks, R. A. Clark, D. A. Cheresh, *ibid.* **264**, 569 (1994); P. C. Brooks *et al*., *Cell* **79**, 1157 (1994); P. C. Brooks *et al*., *J. Clin. Invest.* **96**, 1815 (1995); S. Stromblad, J. C. Becker, M. Yebra, P. C. Brooks, D. A. Cheresh, *ibid.* **98**, 426 (1996).
9. J. E. Meredith, B. Fazeli, M. A. Schwartz, *Mol. Biol. Cell* **4**, 953 (1993); Z. Zhang, K. Vuori, J. C. Reed, E. Ruoslahti, *Proc. Natl. Acad. Sci. U.S.A.* **92**, 6161 (1995).
10. F. Re *et al*., *J. Cell Biol.* **127**, 537 (1994).
11. H. P. McNamee, D. E. Ingber, M. A. Schwartz, *ibid.* **121**, 673 (1993); M. A. Schwartz, C. Lechene, D. E. Ingber, *Proc. Natl. Acad. Sci. U.S.A.* **88**, 7849 (1991); L. E. Dike and D. E. Ingber, *J. Cell Sci.* **109**, 2855 (1996).
12. J. Folkman, *N. Engl. J. Med.* **285**, 1182 (1971); D. Hanahan and J. Folkman, *Cell* **86**, 353 (1996); J. Folkman, K. Watson, D. Ingber, D. Hanahan, *Nature* **339**, 58 (1989); D. Ingber *et al*., *ibid.* **348**, 555 (1990).
13. R. Singhvi *et al*., *Science* **264**, 696 (1994).
14. K. L. Prime and G. M. Whitesides, *ibid.* **252**, 1164 (1991); A. Kumar, H. A. Biebuyck, G. M. Whitesides, *Langmuir* **10**, 1498 (1994); M. Mrksich and G. M. Whitesides, *Trends Biotech.* **13**, 228 (1995).
15. J. M. Folkman and A. Moscona, *Nature* **273**, 345 (1978); D. E. Ingber, *Proc. Natl. Acad. Sci. U.S.A.* **87**, 3579 (1990).
16. J. Folkman *et al*., *Am. J. Pathol.* **130**, 393 (1988); T. Spivak-Kroizman *et al*., *Cell* **79**, 1015 (1994); D. J. Falcone, T. A. McCaffrey, A. Haimovitz-Friedman, J. A. Vergilio, A. C. Nicholson, *J. Biol. Chem.* **268**, 11951 (1993).
17. K. Burridge *et al*., *Annu. Rev. Cell Biol.* **4**, 487 (1988); S. W. Craig and R. P. Johnson, *Curr. Opin. Cell Biol.* **8**, 74 (1996).
18. N. Wang, J. P. Butler, D. E. Ingber, *Science* **260**, 1124 (1993); N. Wang and D. E. Ingber, *Biophys. J.* **66**, 2181 (1994); *Biochem. Cell Biol.* **73**, 327 (1995).
19. A. Maniotis, C. S. Chen, D. E. Ingber, *Proc. Natl. Acad. Sci. U.S.A.* **94**, 849 (1997).
20. E. A. Clarke and J. S. Brugge, *Science* **268**, 233 (1995); M. A. Schwartz, M. D. Schaller, M. H. Ginsberg, *Annu. Rev. Cell Dev. Biol.* **11**, 549 (1995); D. E. Ingber, *Cell* **75**, 1249 (1993); G. E. Plopper, H. P. McNamee, L. E. Dike, K. Bojanowski, D. E. Ingber, *Mol. Biol. Cell* **6**, 1349 (1995); S. Miyamoto, S. K. Akiyama, K. M. Yamada, *Science* **267**, 883 (1995).
21. D. E. Ingber, *Annu. Rev. Phys.* **59**, 575 (1997).
22. L. V. Owens *et al*., *Cancer Res.* **55**, 2752 (1995); S. M. Frisch, K. Vuori, E. Ruoslahti, P. Y. Chan-Hui, *J. Cell Biol.* **134**, 793 (1996).
23. M. D. Schaller *et al*., *Proc. Natl. Acad. Sci. U.S.A.* **89**, 5192 (1992); S. K. Hanks, M. B. Calalb, M. C. Harper, S. K. Patel, *ibid*., p. 8487.
24. D. Stamenovic, J. J. Fredberg, N. Wang, J. P. Butler, D. E. Ingber, *J. Theor. Biol.* **181**, 125 (1996); D. E. Ingber, *J. Cell Sci.* **104**, 613 (1993).
25. D. E. Ingber, J. A. Madri, J. D. Jamieson, *Proc. Natl. Acad. Sci. U.S.A.* **78**, 3901 (1981); D. E. Ingber and J. D. Jamieson, in *Tumor Invasion and Metastasis*, L. A. Liotta and I. R. Hart, Eds. (Nijhoff, The Hague, Netherlands, 1982), pp. 335–357; D. E. Ingber and J. D. Jamieson, in *Gene Expression During Normal and Malignant Differentiation*, L. C. Andersson, C. G. Gahmberg, P. Ekblom, Eds. (Academic Press, Orlando, FL, 1985), p. 13; D. E. Ingber, J. A. Madri, J. D. Jamieson, *Am. J. Pathol.* **12**, 248 (1985).
26. I. MacPherson and L. Montagnier, *Virology* **23**, 291 (1964); M. Stoker, C. O'Neill, S. Berryman, V. Waxman, *Int. J. Cancer* **3**, 683 (1968).
27. S. C. Wittelsberger, K. Kleene, S. Penman, *Cell* **24**, 859 (1981); R. W. Tucker, C. E. Butterfield, J. Folkman, *J. Supramol. Struct. Cell. Biochem.* **15**, 29 (1981); J. Folkman and H. P. Greenspan, *Biochim. Biophys. Acta* **417**, 217 (1975).
28. Human pulmonary microvascular endothelial cells (Clonetics) were cultured in EGM medium (Clonetics) supplemented with 2% fetal calf serum, epidermal growth factor (10 ng/ml), and fibroblast growth factor (FGF) (5 ng/ml). Bovine adrenal capillary endothelial cells were cultured in serum-free, chemically defined medium supplemented with FGF (5 ng/ml) (*4*).
29. We coated beads with FN (Collaborative Biomedical; 50 μg/ml) using carbonate buffer (*18*). Patterned substrates containing islands coated with FN were fabricated by a microcontact printing method (*13, 14*). Briefly, hexadecanethiol [$HS(CH_2)_{15}CH_3$] was printed onto gold-coated substrates with a flexible stamp containing a relief of the desired pattern. The substrate was immersed immediately in 2 mM tri(ethylene glycol)-terminated alkanethiol [$HS(CH_2)_{11}(OCH_2CH_2)_3OH$ in ethanol], which coated the remaining bare regions of gold. When these substrates were immersed in a solution of FN, vitronectin, or type I collagen (50 μg/ml in phosphate-buffered saline), the protein rapidly adsorbed only to the stamped regions. Antibody-coated substrates were prepared by first immersing surfaces in a solution of goat antibody to mouse immunoglobulin G Fc (50 μg/ml) and washed with 1% bovine serum albumin in Dulbecco's modified Eagle's medium before immobilizing the mouse antibodies to integrin $\alpha_v\beta_3$ (1 μg/ml; LM609; Chemicon), β_1 (1 μg/ml; BD15; Biosource), or a combination of the two (0.5 μg/ml each). Cells cultured on substrates with no mouse antibody or antibodies to intracellular proteins did not adhere under these conditions.

30. This work was supported by grants from NIH (HL57669, CA55833, GM30367), the Defense Advanced Research Projects Agency, and the Office of Naval Research; postdoctoral fellowships from the American Cancer Society (M.M.) and the Swiss National Science Foundation (S.H.); and partial salary support (C.S.C.) from the Harvard–MIT Health Sciences Technology Program.

27 December 1996; accepted 7 April 1997

Lamina-Specific Connectivity in the Brain: Regulation by N-Cadherin, Neurotrophins, and Glycoconjugates

Akihiro Inoue and Joshua R. Sanes*

In the vertebrate brain, neurons grouped in parallel laminae receive distinct sets of synaptic inputs. In the avian optic tectum, arbors and synapses of most retinal axons are confined to 3 of 15 laminae. The adhesion molecule N-cadherin and cell surface glycoconjugates recognized by a plant lectin are selectively associated with these "retinorecipient" laminae. The lectin and a monoclonal antibody to N-cadherin perturbed laminar selectivity in distinct fashions. In contrast, neurotrophins increased the complexity of retinal arbors without affecting their laminar distribution. Thus, cell surface molecules and soluble trophic factors may collaborate to shape lamina-specific arbors in the brain, with the former predominantly affecting their position and the latter their size.

Many parts of the vertebrate brain are organized into parallel laminae that bear distinct neuronal subtypes and receive distinct synaptic inputs (*1–3*). In the optic tectum of the chick, for example, most retinal axons terminate in just 3 of 15 laminae (Fig. 1A). Each individual axon arborizes within a single lamina, even though the dendrites of some postsynaptic cells extend through many laminae (*4–6*). The lamina-selective arborization of incoming axons may be a major determinant of specific synaptic connectivity.

To elucidate the mechanisms underlying lamina-specific retinotectal connectivity, we devised a coculture system in which a transverse tectal section was overlaid with a retinal strip, such that neurites from retinal ganglion cells had equal access to all tectal laminae (Fig. 1B). Outgrowth and arborization on these sections reproduced the lamina-selective patterns observed in vivo, implicating local tectal cues in axonal guidance (*5*). Moreover, lamina-selective growth persisted when sections were chemically fixed before retinal strips were added, which implied that some cues are associated with the cell surface and are independent of activity (*5*). We later assessed the distribution of cell adhesion mol-

Department of Anatomy and Neurobiology, Washington University School of Medicine, 660 South Euclid Avenue, Box 8108, St. Louis, MO 63110, USA.

*To whom correspondence should be addressed.